Particle and power balances of hot-filament discharge plasmas in a multidipole device

M-H. Cho, N. Hershkowitz, and T. Intrator
Nuclear Engineering and Engineering Physics, University of Wisconsin-Madison, Madison, Wisconsin 53706-1687

(Received 1 September 1989; accepted for publication 6 December 1989)

This paper considers particle and power balances to estimate the bulk plasma potential of a hot-filament discharge plasma produced in a multidipole plasma device. The bulk plasma potential dependence on positive dc bias applied to an anode is analyzed, and the predicted characteristics of the plasma potential are compared to the experiment. It is shown that the plasma potential can be more positive or more negative than the anode bias potential. When the potential is more negative, a steady-state potential dip in front of an anode is observed using emissive probes with the zero-emission inflection point method. Conditions for the potential dip formation are discussed.

I. INTRODUCTION

Hot-filament discharge plasmas have been widely employed for studying basic plasma phenomena.[1] The addition of multidipole surface magnetic fields at the plasma boundaries has improved the confinement of charged particles and thus enhanced plasma density and uniformity.[2,3] As a result, such multidipole devices can be operated at neutral pressures that are several orders of magnitude lower than in conventional discharge devices. Source characteristics, such as parametric dependencies of plasma parameters, i.e., density, electron temperature, neutral pressure, cusp magnetic field geometry, plasma potential, etc., have been the subjects of many investigations.[2,3]

In this experiment a few movable disk electrodes with known surface area were placed in a multidipole device. They were individually biased to control the charged-particle collections. Grounded electrodes were present at the multidipole cusps. The resulting plasma potential was determined.

In general, the plasma potential is determined by the balance of electron and ion creation and loss, and by the power balance. There are three main charged species in the multidipole device since plasma is produced by a hot-filament discharge. They are isotropic and monoenergetic (at low neutral pressure) primary electrons emitted from the hot filament, Maxwellian plasma electrons, and relatively cold ions ($T_i < 1$ eV and $T_i \ll T_e$, where T_i and T_e denote ion and electron temperatures). Secondary electrons emitted by the energetic primary-electron bombardment have been identified as playing an important role in determining the plasma potential.[4]

The plasma system considered here is shown in Fig. 1 with a sketch of estimated plasma potential profiles. The spatial plasma potential profile is generally considered to have a profile similar to trace A in Fig. 1(b). Plasmas float above the anode potential, a few times T_e/e more positive than the anode bias, thus establishing a weak sheath that limits the electron loss at the anode. This type of weak sheath can be estimated from the particle balance.[4] However, depending on the detailed power balance in the plasma system, a profile similar to trace B in the figure is also possible which shows a potential dip with potential $V_p < V_a$. Here the dip plays the same role in confining plasma electrons as the potential decrease associated with the sheath V_a in the case of the trace A. A potential dip similar to trace B in a dc system has been experimentally observed by Forest and Hershkowitz.[5]

This paper describes the particle and power balances of a bulk plasma in a multidipole device for the estimation of a bulk plasma potential, as well as the plasma sheath potential at the anode, and the condition is analyzed for the potential dip formation at the anode. Comparison is made to the experimental results.

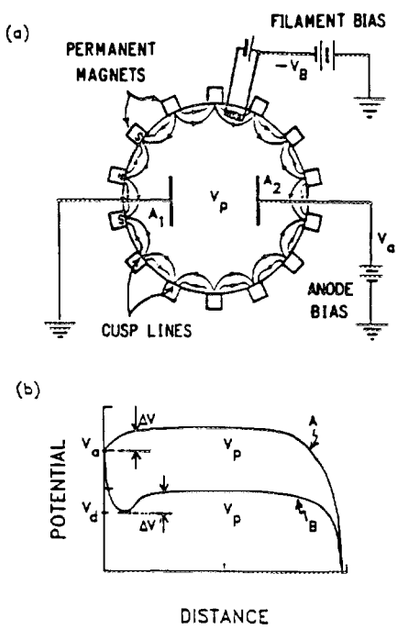

FIG. 1. (a) The plasma system configuration for particle and power balances and (b) possible steady-state plasma potential profiles.

 0021-8979/90/073254-06$03.00

II. PARTICLE AND POWER BALANCES IN A HOT-FILAMENT DISCHARGE PLASMA

A. Particle balance

In a steady-state system, the primary-electron source is the filament discharge current I_d. These primary electrons are lost to ionization processes, nonionizing energy-transfer collisions with neutrals, and to the walls. Balancing sources and losses gives

$$\frac{I_d}{e} = n_p V\left(\frac{1}{\tau_I} + \frac{1}{\tau_W} + \frac{1}{\tau_H}\right), \tag{1}$$

where decay times associated with the losses are

$$\begin{aligned} \tau_I &= (\sigma_I n_0 v_p)^{-1} \quad \text{(for ionization)}, \\ \tau_H &= (\sigma_H n_0 v_p)^{-1} \\ &\quad \text{(for losses due to collisions with neutrals)}, \end{aligned} \tag{2}$$

and τ_w is for losses to the walls and boundaries, n_p is the density of the primary electron, n_0 is the neutral density, σ_I is the ionization cross section, σ_H is the total energy-transfer cross section for electron-neutral collisions, and V is the plasma volume. Electrons are created at the hot filaments by ionization and secondary emission, and lost at the wall cusps and the electrodes. Assuming Maxwellian electrons for the plasma electrons, the balance of plasma electron creation and loss gives

$$\begin{aligned} &I_d/e + n_p V/\tau_I + \delta n_p v_p W_p L_{pc} \\ &\quad = \tfrac{1}{4} n_e v_e (W_e L_c + A_1)\exp(-eV_p/T_e) \\ &\qquad + \tfrac{1}{4} n_e v_e A_2 \exp(-e\Delta V/T_e) + n_p V/\tau_w, \end{aligned} \tag{3}$$

where $v_p = 4.2\times 10^7\sqrt{(2E_p)}$ cm/s with the primary-electron energy E_p in eV, v_e are the speed of the primary and thermal electrons, δ is the secondary-electron emission coefficient by the primary-electron bombardment, A_1 and A_2 [see Fig. 1(a)] are the areas of grounded and positively biased (anode) electrodes, and $\Delta V = V_p - V_d$. L_c is the total cusp length in the system, and L_{pc} is the total cusp length for the primary-electron loss which can differ from L because primary electrons can be lost directly to cusps at the plasma boundary. Note that the filament in Fig. 1(a) is located within the magnetic field between two line cusps, and so the primary leak occurs mainly at the neighboring cusp lines. If the filament is located outside the cusp field, the surface area of the electrodes and other boundaries should also be counted as a leak area. W_p and W_e are the effective leak widths of primary and plasma electrons at the cusp (grounded wall) which are approximately twice the corresponding characteristic widths,[3] i.e., the primary-electron gyroradius (r_p) and the hybrid width (r_h), respectively. The leak widths are

$$\begin{aligned} W_p &= 2r_p = 6.78\sqrt{E_p}\times 10^{-3} \text{ cm} \quad (\text{for } B = 1 \text{ kG}), \\ W_e &= 2r_h = 4\sqrt{(r_e r_i)}, \end{aligned} \tag{4}$$

where E_p is the energy of the primary electron. If we assume the potentials shown in Fig. 1(b) (trace B) as $eV_p/T_e \gg 1$ and $\Delta V \sim T_e/e$, that is, the grounded wall will not contribute to the plasma electron loss, then Eq. (3) can be approximated as

$$\begin{aligned} &I_d/e + n_p V/\tau_I + \delta n_p v_p W_p L_{pc} \\ &\quad \simeq \tfrac{1}{4} n_e v_e A_2 \exp(-e\Delta V/T_e) + n_p V/\tau_w. \end{aligned} \tag{5}$$

Ions are lost to the grounded boundary (i.e., the grounded electrode at the wall cusps) in the plasma. Note that the biased electrode potential V_a is more positive than V_p, and so there is no ion loss at the anode since $e(V_a - V_d)/T_i \gg 1$, where V_d is the potential at the dip shown in Fig. 1(b) (trace B). The ion balance becomes

$$n_p V/\tau_I = \tfrac{1}{2} n_i c_s (W_i L_c + A_1), \tag{6}$$

where c_s is the ion-sound velocity. It has been observed experimentally that the effective ion-leak width W_i is approximately $4W_e$.[3]

Using Eqs. (1), (5), and (6), one can solve for ΔV. Using the condition of charge neutrality, i.e., $n_e + n_p + n_{se} \simeq n_i$, the solution is

$$\begin{aligned} \frac{e\Delta V}{T_e} &\simeq \ln\left(\frac{v_e A_2}{2c_S(W_i L_c + A_1)}\right) \\ &\quad - \ln\left(2 + \frac{\tau_I}{\tau_H} + \frac{\delta W_p L_{pc}}{\sigma_I n_0 V}\right). \end{aligned} \tag{7}$$

If we consider the trace A with the same assumptions as for Eq. (7), ΔV will be described by the same expression with the denominator replaced by $2c_s(W_i L_c + A_1 + A_2)$ in the first term of the right-hand side (RHS). As one can see from Eq. (7), the addition of area A_2 in the denominator will not affect the result significantly. For the case of trace A, the plasma potential is simply $V_p = V_a + \Delta V$. The plasma potential for trace B cannot be determined by Eq. (7) alone.

B. Power balance

The power balance provides an additional relationship that must be satisfied and allows the determination of V_p for trace B. The power removed from the system is carried away by the charged particles lost at the plasma boundaries. This has to be balanced with the input power which is supplied by the primary electrons from the filament discharge $E_p I_d/e$. Note that the primary-electron energy E_p equals $e(V_p + V_B)$ since the filament is biased at $-V_B$ and the primary electrons are accelerated as they enter into the plasma having potential V_p.

Biasing the anode more positive increases the potential energy of the system, but it also can enhance electron loss from the system. Using the particle loss at the boundaries discussed above, the electron and ion power flow to the boundary, Q_e and Q_i, can be written

$$\begin{aligned} Q_e &\simeq [2T_e + e(V_a - V_d)]\tfrac{1}{4} n_e v_e A_2 \exp(-e\Delta V/T_e) \\ &\quad + eV_a \tfrac{1}{4} n_{se} v_{se} A_2 + E_p (n_p V/\tau_w), \end{aligned} \tag{8}$$

$$Q_i \simeq (eV_p)\tfrac{1}{2} n_i c_s (W_i L_c + A_1), \tag{9}$$

where n_{se} is for the density of secondary electrons emitted by the primary-electron bombardment, and n_p is the primary-electron density. The secondary electrons emitted at the wall (grounded) become monoenergetic with energy approximately eV_p, because they are accelerated by the wall sheath [the second term in the RHS of Eq. (8)]. The $2T_e$ in the RHS of Eq. (8) comes from the fact that for the Maxwellian

distribution, the energy flux in the x direction, is just $2T_e$ times the particle flux in the x direction,[6] and they acquire the energy of $e(V_a - V_d)$ as they accelerate toward the anode after passing the dip. The eV_p in the RHS of Eq. (9) comes from the fact that ions falling to the sheath gain energy of eV_p. The ions are assumed to be cold ($T_i \ll 1$ eV). It is assumed that each primary electron makes only a single ionizing collision and the secondary electrons do not contribute to ionization. Other energy-loss processes, such as charge exchange, radiation, etc., are also neglected.

The power balance is

$$\alpha E_p I_d / e = Q_e + Q_i, \tag{10}$$

where α denotes the fraction of the effective power coupled to the plasma. Note that some emitted electrons go directly to the cusp of the source. Substituting Eqs. (8) and (9) into Eq. (10) and arranging the resulting equation for V_p gives

$$\left[I_e + \alpha I_d - I_i\left(1 + \frac{\tau_I}{\tau_w}\right)\right] V_p \simeq V_a (I_e + I_{se}) + \Delta V I_e + \frac{2T_e}{e} I_e - V_B \left(\alpha I_d - I_i \frac{\tau_I}{\tau_w}\right), \tag{11}$$

where

$$I_e = A_2 \Gamma_e = \tfrac{1}{4} e n_e v_e A_2 \exp(-e\Delta/T_e),$$
$$I_i = (A_1 + W_i L_e)\Gamma_i = \tfrac{1}{2} e n_i c_s (W_i L_e + A_1),$$
$$I_{se} = A_2 \Gamma_{se} = \tfrac{1}{4} e n_{se} v_{se} A_2,$$
$$\Delta V = V_p - V_d.$$

The results derived here are approximate because only one-dimensional characteristics are considered, and the variations of electron and ion distribution functions are simplified by assuming Maxwellian distribution for electrons and cold ions. If we neglect the power loss by the secondary electrons in Eq. (11), and assume $\tau_I/\tau_w \sim 1$ (valid near 10^{-4} Torr) and $I_e \gg (\alpha I_d - 2I_i)$ with $T_e \gg T_i$, then V_p is approximately

$$V_p \sim V_a + \Delta V + \frac{2T_e}{e} - V_B \frac{\alpha I_d}{I_e}. \tag{12}$$

Equation (12) indicates that V_p linearly follows the anode voltage with a slope of approximately 1.0. Equation (12) also shows that V_p becomes more negative for the fixed V_a as the fraction of the primary-electron current to the electron-loss current increases. The last term in Eq. (12) also shows that V_p becomes more negative as V_B (magnitude of the filament bias) increases. However, varying the primary-electron energy affects the ionization, the secondary-electron emission, and other plasma parameters as well, and so it is not as simple of a problem as it appears to estimate the effect of V_B on V_p from Eq. (12).

So far, the power balance for trace B has been considered. However, based on the preceding discussion, it must be that the power balance cannot be satisfied when $V_p > V_a$ (i.e., for the case of trace A). For the simplicity, we consider the bulk plasma electrons and ions. Then Eqs. (8) and (9) for curve A become

$$Q_i = V_p I_i, \tag{8'}$$

$$Q_e = (2T_e/e) I_{e0} \exp[-e(V_p - V_a)/T_e], \tag{9'}$$

where

$$I_i = \tfrac{1}{2} e n_i c_s (A_1 + A_2 + A_w),$$
$$I_{e0} = \tfrac{1}{4} e n_e v_e A_2.$$

The power balance, $P_{in} = Q_i + Q_e$, using Eqs. (8') and (9'), gives

$$T_e \sqrt{\frac{m_i}{m_e}} \frac{A_2}{A_1 + A_2 + A_w} \exp\left(\frac{-e(V_p - V_a)}{T_e}\right) = \frac{eP_{in}}{I_i} - eV_p, \tag{13}$$

where $P_{in} = \alpha E_p I_d / e$ is the input power as in Eq. (10). For a fixed input power, one can solve Eq. (13) for V_p graphically. Figure 2 shows the graphic solution, where $y_1(eV_p)$ is the left-hand side (LHS) and $y_2(eV_p)$ is the RHS of the Eq. (13). The solution exists for $V_p > V_a$, only when y_1 and y_2 intersect (the region above the solid lined y_2). The particle balance determines one solution out of two intersection points. Depending upon the input power and the ion-loss rate, as one can see in the RHS of Eq. (13), Eq. (13) may not have a solution, which suggests that the assumption of $V_p > V_a$ to derive Eq. (13) is not valid for our arbitrary plasma system.

III. EXPERIMENTAL OBSERVATIONS

It was found that the bulk plasma potential can be controlled by introducing a biased conducting boundary, i.e., an additional anode, in a plasma. The surface area of this additional anode must be relatively large so that the dominant loss of the plasma electrons occurs at the anode. When a positive voltage (with respect to ground) is applied to an anode, plasmas, in general, float above the anode voltage such that the anode sheath limits the electron loss as a part of the balancing process. However, as described earlier in Sec. II, situations exist where the plasma potential stays negative with respect to the anode potential.[5]

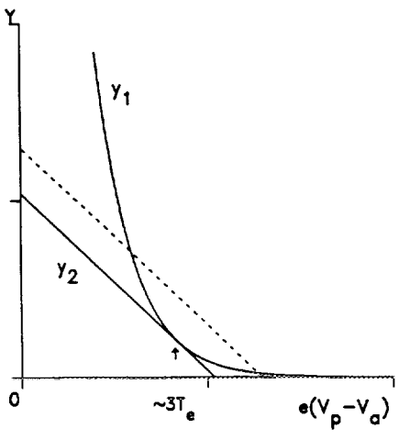

FIG. 2. Graphical solution for the power balance [see Eq. (13)].

Experiments were carried out in a multidipole device which was built using a 40-ℓ stainless-steel soup pot (35.5-cm-diam and 40.5-cm-high cylinder). Fourteen columns of permanent magnets were equally spaced around the circumference. Top and bottom plates were also covered with permanent magnet strips which produce multidipole surface magnetic fields covering the whole chamber (total length of line cusp is approximately 800 cm). Plasmas were produced by hot-filament discharge. Typical plasma parameters were $T_e \sim 3$ eV, $T_i \sim 0.3$ eV, and $n_e \sim 1\times 10^9$ cm^{-3} at neutral pressure of argon gas $\sim 1\times 10^{-4}$ Torr. Planar Langmuir probes (0.7 cm in diameter) were used for plasma density and the electron temperature measurements. The plasma potential is measured using an emissive probe based on the zero-emission inflection point method, which whch is described in detail elsewhere.[7]

The anode introduced in the multidipole device was made out of Cu or stainless-steel plates with a diameter of 7.5 cm and thickness of 0.1 cm, and the back side was either covered with an insulating layer (ceramic paste or mica plate) or left exposed to the plasma. The arrangements of the anode, grounded electrode, and the filament are shown schematically in Fig. 1(a), and they are all movable to accommodate different boundary conditions, e.g., trapped and untrapped primary electrons, a bare metal anode, an anode partially covered with an insulating layer, etc. Here "trapped" means that the hot filament is located inside one of the cusp magnetic fields, as shown in Fig. 1(a), such that the emitted primary electrons are confined in the magnetic field lines and most of them do not get directly into the bulk plasma region, and "untrapped" means that the filament is located well inside the chamber so that the primary electrons bounce around reflected (by the cusp magnetic field) in the bulk plasma region.

When the primary electrons are trapped, one can observe a bluish purple column (for argon gas) confined along the line cusp where the filament is located. The glowing column tends to have a much higher plasma density (approximately 10 times higher than that of the bulk plasma in the middle of chamber at an argon neutral pressure of $\sim 2\times 10^{-4}$ Torr). This plasma, isolated from the bulk plasma by the cusp magnetic field, acts as an electron supply source, i.e., charged particles diffuse into the bulk plasma region by collisions because of the density gradient, and $\nabla\mathbf{B}\times\mathbf{B}$ drift.

When a bare anode (without any insulating layer) bias was varied from 0 to 50 V, the plasma potentials closely followed the anode voltage (slope ~ 1.0 for V_a above 10 V) shown in Fig. 3 for a few different neutral-pressure cases with the filament located in the bulk plasma region (untrapped). Figure 4 shows the trapped primary-electron case. The solid straight line in the figures represents the line $V_p = V_a$ for comparison. We find that the plasma potential becomes more negative as the neutral pressure decreases or as the energy of the primary electron decreases. However, the change of the plasma potential is within a few volts (for the anode bias up to 50 V) except when the primary-electron density is a signficant fraction of the plasma density (when there can be more than a 10 V drop as seen in the lowest trace

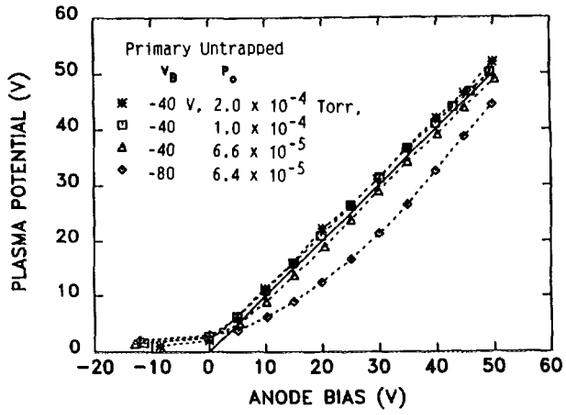

FIG. 3. Bulk plasma potential vs anode voltage for the untrapped primary-electron case. Plasma parameters at $V_a = 50$ V are $T_e \sim 2$ eV, $n_e \sim 1\times 10^9$ cm^{-3} for $P_0 > 1\times 10^{-4}$ Torr, and $T_e \sim 4$ eV, $n_e \sim 5\times 10^8$ cm^{-3} for $P_0 < 1\times 10^{-4}$ Torr.

in Fig. 3). The plasma potential in Fig. 4 (trapped) is a few volts lower than the plasma potential in Fig. 3 (untrapped) for a pressure greater than 1×10^{-4} Torr when the anode is biased above 10 V. The reason for the more negative potential in the trapped primary case is that the plasma electrons produced in the cusp region (biased at the ground), where the filament is located, acquire energy when they diffuse into the bulk plasma region (positively biased), and so they behave like energetic primary electrons.

When the anode with the back side covered with an insulating area was biased such that the part of the anode surface was at the floating potential, the plasma potentials were generally more negative than the anode voltage. Figure 5 shows the change in the plasma potential (~ 10 V at 50-V bias) found using two different insulating layers (mica plate and ceramic paste) for untrapped primary electrons. These

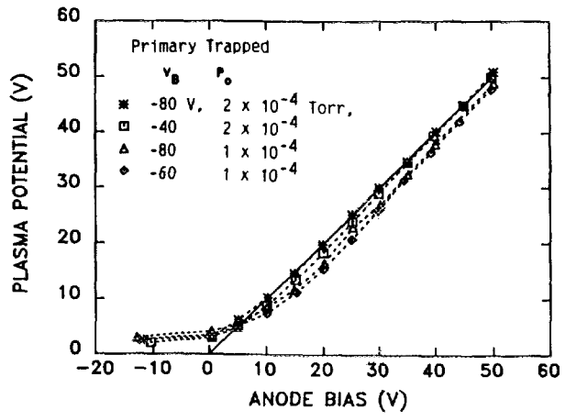

FIG. 4. Bulk plasma potential vs anode voltage for the trapped primary-electron case ($T_e \sim 3$ eV, $n_e \sim 7\times 10^8$ cm^{-3} at $V_a = 50$ V).

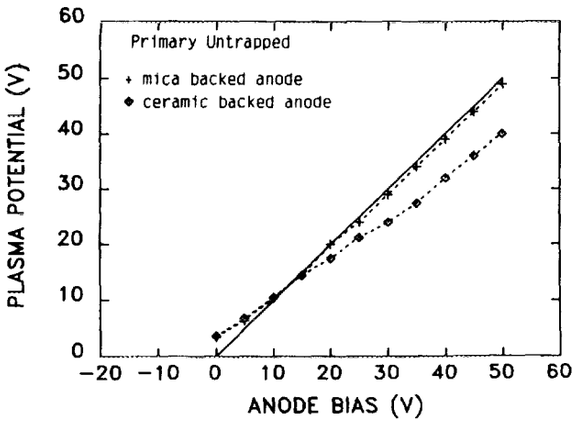

FIG. 5. Bulk plasma potential vs anode voltage. The back side of the anode surface (7.5-cm-diam Cu disk) is covered with an insulating layer (mica and ceramic layers are tested). Plasma parameters at $V_a = 50$ V are $T_e \sim 3$ eV, $P_0 \sim 1.5 \times 10^{-4}$ Torr, and $n_e \sim 1.4 \times 10^9$ cm^{-3}.

data indicate the importance of the surface condition. Note that mica has a secondary-electron emission coefficient of $\delta_{max} \sim 2.4$ at 350 eV,[8] and the ceramic paste is expected to have higher δ.

It has been observed that the spatial plasma potential profiles have a potential dip near the anode, typically $V_p - V_d = 2$–3 V, when the bulk plasma potentials are negative with respect to the anode voltage, i.e., when $(V_a - V_p) > 3$ V. The dip is apparent in the lowest trace in Figs. 3 and 5. The size of the potential dip, as a function of plasma potential, was observed to be constant within the resolution of measurement.

IV. DISCUSSION

The expression of plasma potential (V_p), derived in an earlier section for the case of trapped primary electrons [see Eq. (12)], qualitatively agrees with the observed dependencies, that is, the linear dependence on the anode voltage (V_a), and the plasma potential becomes more negative as the fraction of the primary-electron current to the electron-loss current increases. However, many parameters in the equation, i.e., I_d, I_a, n_e, σ_I, δ, etc., are all interrelated and cannot be controlled separately in the experiment. The simplified model described here does not include the detailed dependencies.

The plasma potential change due to the plasma density change can be understood qualitatively as follows. To change plasma density in a hot-filament discharge system, one has to vary either neutral density or the filament discharge current (or both). When one chooses the former method, for example, lowering the neutral pressure to decrease the plasma density, the ratio of the primary-electron density to the plasma-electron density increases due to the decreased collisionality. This is equivalent to the situation which occurs when one adds extra primary electrons in the system. Since the bulk of plasma maintains quasineutrality of the charge, the bulk plasma potential has to be more negative to enhance the plasma electron loss. However, when the discharge current is varied with the neutral pressure fixed, the plasma potential does not change because the fraction of the primary-electron density stays constant (note that the plasma density is linearly proportional to the filament discharge current).

Using plasma parameters for the lower trace in Fig. 5, Eq. (7) gives $e\Delta V/T_e = e(V_p - V_d)/T_e \sim 0.82$, or $\Delta V \sim 2.5$ V, and this agrees closely to the measured potential dip. As one can see from Eq. (7), this result is insensitive to the change of the primary-leak area [the last term in Eq. (7)], but sensitive to the anode area (the numerator in the first term). For example, again using the above parameters, when the anode area is $A_2 \leqslant 20$ cm, the result becomes negative, i.e., $V_d > V_p$, and the analysis breaks down. This indicates that the electrode can no longer control the bulk plasma potential in the system and is similar to the case of a positively biased Langmuir probe. For the profile similar to trace A in Fig. 1(b), the ion leak also occurs at the anode; thus the ion leak area in Eq. (6) should be changed to include this (the denominator of the first term in the RHS). However, as one can see in the equation, the difference in $e\Delta V/T_e$ is very small. From the particle balance there is no way of knowing the plasma potential V_p when V_p has the spatial profile similar to the trace B (i.e., $V_p < V_a$), because the potential is referenced at the plasma potential.

Again using the same parameters as above [Eq. (12)], i.e., the power balance equation, gives

$$V_p \sim 76 - 50\alpha \ \text{(V)}.$$

This gives $V_p \sim 40$ V when $\alpha \simeq 0.7$. Note that the parameter α was chosen as an indication of the primary-electron effectiveness for the production of plasma.

V. CONCLUSION

The model presented in this paper does not describe the system exactly, but shows that one can get a rough estimate of the plasma potential and/or plasma parameter dependence of the plasma potential for a given plasma system (steady state) by properly applying the particle and power balances.

Based on the discussions and the examples given here, it can be concluded that the potential dip, which occurs in front of the positively biased anode in a steady-state hot-filament discharge plasma, is the result of the charged-particle production and loss balance with the condition $V_p < V_a$, which is determined by the balance of the input power and the power carried away by the charged particles. The condition $V_p < V_a$ can be obtained by the continuous supply of extra electrons or continuous removal of ions from the plasma system.

ACKNOWLEDGMENT

This work was supported by NSF Grant No. ECS-8704529.

[1] I. Alexeff, W. D. Jones, and K. E. Lonngren, Phys. Rev. Lett. **21**, 878 (1968).
[2] K. N. Leung, N. Hershkowitz, and K. R. Mackenzie, Phys. Fluids **19**,

1045 (1976); N. Hershkowitz, K. N. Leung, and T. Romesser, Phys. Rev. Lett. **35**, 277 (1975); R. Limpaecher and K. R.Mackenzie, Rev. Sci. Instrum. **44**, 726 (1973).
[3]K. N. Leung, T. K. Samec, and A. Lamm, Phys. Lett. **51A**, 490 (1975).
[4]C. Chan, T. Intrator, and N. Hershkowitz, Phys. Lett. **91A**, 167 (1982).
[5]C. Forest and N. Hershkowitz, J. Appl. Phys. **60**, 1295 (1986).
[6]P. C. Stangeby, in *Physics of Plasma-Wall Interactions in Controlled Fusion*, edited by D. E. Post and R. Behrisch (Plenum, New York, 1986), pp. 41–98.
[7]J. R. Smith, N. Hershkowitz, and P. Coakley, Rev. Sci. Instrum. **50**, 210 (1979); N. Hershkowitz, in *Plasma Diagnostics*, edited by O. Auciello and D. L. Flamm (Academic, Orlando, FL, 1989).
[8]*Handbook of Chemistry and Physics*, 66th ed. (CRC, Cleveland, OH, 1985–1986), p. E-365.